Available online at www.sciencedirect.com
ScienceDirect
Polymer 48 (2007) 5940–5949
polymer
www.elsevier.com/locate/polymer

Efficiency of graft copolymers as compatibilizers for immiscible polymer blends

Cai-Liang Zhang [a,b], Lian-Fang Feng [a,b,**], Xue-Ping Gu [a,b], Sandrine Hoppe [b], Guo-Hua Hu [b,c,*]

[a] State Key Laboratory of Chemical Engineering, College of Materials Science and Chemical Engineering, Zhejiang University, Hangzhou 310027, China
[b] Laboratory of Chemical Engineering Sciences, CNRS-ENSIC-INPL, 1 rue Grandville, BP 20451, 54001 Nancy, France
[c] Institut Universitaire de France, Maison des Universités, 103 Boulevard Saint-Michel, 75005 Paris, France

Received 22 January 2007; received in revised form 13 June 2007; accepted 20 July 2007
Available online 26 July 2007

Abstract

This work was aimed at studying the emulsification efficiency of graft copolymers and the effect of feeding mode on the emulsification efficiency using the emulsification curve approach. The blends were composed of polystyrene (PS) and polyamide 6 (PA6). PS was always the matrix and PA6 the dispersed phase. A series of graft copolymers of PS and PA6, denoted as PS-*g*-PA6, with different molecular structures were used as emulsifiers. Feeding mode had a very significant effect on the size of the dispersed phase domains at short mixing time and its effect decreased or became negligible at long mixing time. This indicates that feeding mode affected mostly the time necessary for the PS-*g*-PA6 emulsifier to reach and emulsify the PS/PA6 interfaces. The molecular structure of the PS-*g*-PA6 graft copolymer also had a profound effect on its emulsification efficiency. The longer the PA6 grafts (from 1.7 to 5.1 kg/mol), the higher the emulsification efficiency. On the other hand, the number of PA6 grafts had little effect on the emulsification efficiency when the PA6 grafts were short (1.6–1.7 kg/mol). The effect of the blend composition was also investigated.

Keywords: Polymer blends; Emulsification curve; Graft copolymer

1. Introduction

It is a common practice to prepare new polymer materials by blending different polymers. However, a vast majority of polymers are mutually immiscible and thermodynamically unstable. Therefore, block or graft copolymers whose segments are chemically identical to or having affinity with the polymer components are often used as emulsifiers (also called interfacial modifiers or compatibilizers) to reduce the interfacial tension, promote the dispersion of one phase in another and stabilize resulting blends [1–3]. Favis and co-workers carried out extensive studies on the use of emulsification curves to evaluate the efficiency of copolymers as emulsifiers [4–9]. The latter essentially follows the evolution of the dispersed phase size with the copolymer concentration. It is often characterized by an initial significant decrease in the size of the dispersed phase domains with the addition of the copolymer followed by a leveling-off at higher copolymer concentrations. The shape of the emulsification curve depends both on the molar mass and molecular architecture of the copolymer and on the processing conditions.

Table 1 gathers some literature results on the effects of the molar mass and molecular architecture of a copolymer on its emulsification efficiency for polymer blends. The emulsification efficiency followed the order: tapered biblock > conventional diblock > triblock; a smaller molar mass > a higher

* Corresponding author. Laboratory of Chemical Engineering Sciences, CNRS-ENSIC-INPL, 1 rue Grandville, BP 20451, 54001 Nancy, France. Tel.: +33 383175339; fax: +33 383322975. Laboratory of Chemical Engineering Sciences, CNRS-ENSIC-INPL, 1 rue Grandville, BP 20451, 54001 Nancy, France.
** Corresponding author. State Key Laboratory of Chemical Engineering, College of Materials Science and Chemical Engineering, Zhejiang University, Hangzhou 310027, China.
E-mail addresses: fenglf@zju.edu.cn (L.-F. Feng), hu@ensic.inpl-nancy.fr (G.-H. Hu).

0032-3861/$ - see front matter © 2007 Elsevier Ltd. All rights reserved.
doi:10.1016/j.polymer.2007.07.042

molar mass. Table 2 gathers some literature results on the effect of feeding mode on the morphology of polymer blends. It is seen that the effect of feeding mode could also be very important but appeared to be blend specific. In other words, a feeding mode that was most efficient for a blend might not necessarily be so for another one, even for the same blend of a different composition.

The aforementioned studies were focused mainly on the emulsification efficiency of block copolymers, on one hand (Table 1); and on the effect of feeding mode on reactive polymer blends, on the other hand (Table 2). The work reported in this paper was aimed at studying the emulsification efficiency of graft copolymers and the effect of feeding mode associated with such type of copolymer as emulsifier. The blend system was composed of polystyrene (PS) and polyamide 6 (PA6). PS was always the matrix and PA6 the dispersed phase. A series of graft copolymers of PS and PA6, denoted as PS-*g*-PA6, with different molecular structures and/or molar masses were used as emulsifiers.

2. Experimental

2.1. Materials

Table 3 gathers selected characteristics of PS and PA6 used in this work.

The PS-*g*-PA6 graft copolymers were obtained by the anionic polymerization of ε-caprolactam (CL) onto a random copolymer of styrene (St) and 3-isopropenyl-α,α-dimethylbenzene isocyanate (TMI), denoted as PS-*co*-TMI. Details on the polymerization principle and procedures can be found elsewhere [16–19]. Table 4 shows some of the characteristics of PS-*co*-TMI used for the polymerization.

Table 1
Literature results on the emulsification efficiency of copolymers

Blend	Type of copolymer	Emulsifying effect of the copolymer
PS/EPR (90/10) [4]	SEBS (50–174 kg/mol; 28.6–33.3% PS); SBu (66–176 kg/mol; 30.0–45.4% PS)	Molar mass: little effect. Chemical composition: big effect. SEBS (without unsaturation) was more efficient than SBu (with unsaturation) because the saturated EB middle block of SEBS had higher affinity with EPR than the unsaturated Bu
SPS/EPR [5,6]	SEP (85–130 kg/mol; 31% PS) for SPS/EPR (75/25); SEBS (50–74 kg/mol; 30–33% PS) for SPS/EPR (80/20)	The smaller the molar mass, the higher the emulsification efficiency because of higher diffusivity
PS/EPR (80/20) [7]	SBu (symmetrical: 63 kg/mol, 53% PS; asymmetrical: 67 kg/mol, 30% PS)	The symmetrical one was more efficient than the asymmetrical one because the latter had higher tendency to form micelles
PS/EPR [8]	Diblock: SEB (67 kg/mol; 30% PS); triblock: SEBS (70 kg/mol; 29% PS)	Diblock was more efficient than triblock for PS/EPR (80/20) and less efficient for PS/EPR (90/10) because the latter had higher tendency to form micelles
LDPE/PS (80/20) [9]	Diblock: PS-*b*-PB (35–35 kg/mol); tapered diblock: PS-*b*-P(S-*co*-B)-*b*-PB (23–19–28 kg/mol); triblock: PS-*b*-P-(S-*co*-B)-*b*-PB (75–35–75 kg/mol)	The tapered diblock copolymer was the most efficient. Unlike the tapered diblock, the diblock was partly located in PS and the triblock micellized in LDPE

Table 2
Literature results on the effects of feeding mode on the morphology of reactive blends

Blend system	Feeding mode	Morphology
PA6/EPR/EPR-*g*-MA (80/15/5) [10]	One-step: all the blend components were charged to the mixer at the same time; two-step: EPR and EPR-*g*-MA charged first and PA6 10 min later	Two-step much better than one-step
PA6/PE/PE-*co*-acid [11]	One-step: all the blend components were charged to the mixer at the same time; two-step: PE-*g*-acid mixed first with the dispersed phase and then the matrix	Two-step was better than one-step for PA6/PE/PE-*g*-acid (90/10/0.5) and opposite result for PA6/PE/PE-*g*-acid (10/90/0.5)
PA6/PP/PP-*g*-MA [12]	One step: all the blend components were charged to the mixer at the same time; two-step 1: PP and PP-*g*-MA charged first and then PA6; two-step 2: PA6 and PP-*g*-MA charged first and then PP	Similar morphologies for the one step and two-step 1 and finest morphology for the two-step 2
PA6/PP/PP-*g*-MA [13]	Two-step: PP was first functionalized with MA in an extruder (first step), and PA6, PP and the resulting PP-*g*-MA were blended in a separate extrusion step; one-step: PP was functionalized with MA in the first part of the extruder and PA6 and PP were charged to the extruder downstream	Both two-step and one-step processes yielded similar morphologies and mechanical properties provided that in the one-step process monomer residues were removed in an efficient manner
PBT/PP/PP-*g*-GMA [14,15]	Two step: PP was first functionalized with GMA (glycidyl methacrylate) in an extruder (first step), and PBT, PP and the resulting PP-*g*-GMA were blended in a separate extrusion step; one-step: PP was functionalized with GMA in the first part of the extruder and PBT and PP were charged to the extruder downstream	Both two-step and one-step processes yielded similar morphologies and mechanical properties provided that in the one-step process monomer residues were removed in an efficient manner

Table 3
Selected characteristics of PS and PA6 used in this work

	Number-average molar mass[a] (M_n, kg/mol)	Mass average molar mass[a] (M_w, kg/mol)	Supplier
PS	101.3	228.8	Yangzi-BASF Styrenics Co., Nanjing, China
PA6	19.4	49.4	UBE Nylon Ltd., Thailand

[a] Molar masses measured by size exclusion chromatography (SEC) using PS standards for the calibration and tetrahydrofuran (THF) as the eluent. PA6 was first *N*-trifluoroacetylated prior to the SEC measurement. An UV detector at 238 nm was used for the SEC measurement.

Table 4
Selected characteristics of the copolymer PS-*co*-TMI

PS-*co*-TMI	M_n[a] (kg/mol)	M_w[a] (kg/mol)	TMI content in PS-*co*-TMI[b] (wt.%)
PS-*co*-TMI1	36.9	68.0	1.0
PS-*co*-TMI4	33.3	97.0	4.0

[a] Molar masses measured by SEC using PS standards for the calibration and THF as the eluent.
[b] TMI contents measured following a method reported in the literature [19].

The isocyanate moieties of PS-*co*-TMI acted as initiating centers from which PA6 grafts grew in the presence of a catalyst like sodium caprolactam (NaCL). Table 5 shows selected characteristics of four as-synthesized PS-*g*-PA6 graft copolymers used in this work. It is noted that none of them was a pure PS-*g*-PA6 graft copolymer but a mixture of a pure PS-*g*-PA6 graft copolymer, homopolyamide 6 and non-polymerized CL monomer residue (<5%). The percentage of the pure graft copolymer in the as-synthesized graft copolymer varied between 51.4% (PS-*g*-PA6d) and 88.5% (PS-*g*-PA6a). The first three graft copolymers had the same PS backbone and the same number of PA6 grafts with different lengths. The fourth graft copolymer, PS-*g*-PA6d, differed from the first three in that the number of the PA6 grafts per PS backbone was not 6.6 but 1.8. The molar masses of the homopolyamide 6 in the as-synthesized products were 14.1, 18.9 and 19.2 kg/mol for PS-*g*-PA6a, PS-*g*-PA6b and PS-*g*-PA6c, respectively, and were very close to that of PA6 used as the dispersed phase of the blend (19.4 kg/mol). Therefore, it was considered as a part of the dispersed phase.

2.2. Blending process

A Haake torque rheometer (HBI system 90) was used as a mixer to study the effect of feeding mode on the morphology and the emulsification efficiency of the four PS-*g*-PA6 graft copolymers for PS/PA6 blends. It was equipped with a mixing chamber of 50 ml in capacity and two rotors inside the mixing chamber. The concentration of the as-synthesized PS-*g*-PA6 graft copolymer in the blends was 2.5%, 5%, 7.5%, 10%, 15%, 20% or 30% with respect to the dispersed phase (PA6). In what follows, it will systematically be converted to an equivalent pure PS-*g*-PA6 graft copolymer concentration. Table 6 shows the compositions of the blends studied in this work. Prior to the blending, PS, PA6 and PS-*g*-PA6 were dried in a vacuum oven at 80–90 °C for 12 h. During the drying process, the non-polymerized CL monomer residue was removed to a very large extent. The dried blend components were fed to the mixer in a one-step or two-step feeding mode. The mixer was preheated at 230 °C and the two rotators inside the mixer rotated in opposite directions either at 65 or 130 revolutions per minute (rpm) to ensure mixing. Samples were taken from the mixing chamber after prescribed time intervals (2–14 min) and were then quenched in liquid nitrogen to freeze-in their morphologies.

2.3. Rheological characterization

An advanced rheometric expansion system (ARES, TA Instruments, USA) was used to characterize the rheological

Table 5
Selected characteristics of the as-synthesized PS-*g*-PA6 graft copolymers

Copolymer designation	Percentage of PS-*g*-PA6 (%)	Composition of PS-*g*-PA6		Number of PA6 grafts per PS backbone	M_n (kg/mol)	
		PS backbone	PA6 grafts		PS backbone	Each PA6 graft
PS-*g*-PA6a	88.5	75.3	24.7	6.6	33.3	1.7
PS-*g*-PA6b	68.6	69.4	30.6	6.6	33.3	2.2
PS-*g*-PA6c	57.5	49.7	50.3	6.6	33.3	5.1
PS-*g*-PA6d	51.4	92.6	7.4	1.8	36.9	1.6

PS-*g*-PA6a, PS-*g*-PA6b and PS-*g*-PA6c were synthesized using PS-*co*-TMI4 and PS-*g*-PA6d using PS-*co*-TMI1.

Table 6
Composition of uncompatibilized and compatibilized blends

Blend system PS/PA6/PS-*g*-PA6	Type of PS-*g*-PA6	Percentage of the equivalent pure PS-*g*-PA6 with respect to the dispersed phase (*x*)							
90/10/*x*	PS-*g*-PA6b	0	1.7	3.4	5.1	6.9	10.3	13.7	20.6
80/20/*x*	PS-*g*-PA6a	0	2.2	4.4	6.6	8.9	13.3	17.7	26.6
	PS-*g*-PA6b	0	1.7	3.4	5.1	6.9	10.3	13.7	20.6
	PS-*g*-PA6c	0	1.4	2.9	4.3	5.8	8.6	11.5	17.3
	PS-*g*-PA6d	0	1.3	2.6	3.9	5.1	7.7	10.3	15.4
70/30/*x*	PS-*g*-PA6b	0	1.7	3.4	5.1	6.9	10.3	13.7	20.6

behavior of the pure polymer components and their blends. The dynamic mode was used to measure the complex viscosity as a function of frequency. The samples were disks of 2.5 cm in diameter and about 0.2 cm in thickness. The test was performed within the frequency region from 100 to 0.1 rad/s.

2.4. Characterization of blend morphologies

A scanning electron microscopy (SEM) of FEI SIRION was used to characterize the blend morphologies. Before the SEM observations, samples were first fractured in liquid nitrogen. The fractured surfaces were then immersed in formic acid at room temperature for 12 h in order to remove the dispersed phase domains (PA6). They were dried for 12 h in the vacuum oven at 80 °C and then gold sputtered. The voltage for the SEM was 5.0 kV.

The diameter of the dispersed phase domains was measured using a semi-automatic image analysis method. It was characterized by volume average particle diameters, d_v, defined by

$$d_v = \frac{\sum n_i d_i^4}{\sum n_i d_i^3}$$

For each blend, at least 500 particles were counted for statistically meaningful values of d_v.

The morphology of some of the PS/PA6/PS-*g*-PA6 blends was also characterized by transmission electron microscopy. Prior to the TEM analysis, specimens were stained in the following manner. They were microtomed into films of less than 100 nm thick. They were then placed on a drop of 2% phosphotungstic acid solution for 30 min at 50 °C using a specimen grid. Thereafter they were rinsed three times with distilled water.

3. Results and discussion

3.1. Rheology

Fig. 1 shows the complex viscosity at 230 °C of PS, PA6 and their blends with mass compositions of 50/50, 70/30 and 80/20 as a function of frequency. As expected, at low frequency the complex viscosities of the PS/PA6 blends were in between those of PS and PA6 and at high frequency they were close.

3.2. Effect of feeding mode

Table 7 shows four different feeding modes that were designed to study the effect of feeding mode on the morphology. Feeding mode 1 was one-step feeding and the other three were two-step feedings. Fig. 2 compares the four feeding modes in terms of the evolution of the dispersed phase domain size as a function of the equivalent pure PS-*g*-PA6b concentration–emulsification curve for the PS/PA6 (80/20) blend for two different rotation speeds of the rotors. For both rotation speeds, when the PS-*g*-PA6 concentration was higher than 10% of PA6, the PA6 particle size followed the order: feeding mode 2 < feeding mode 1 < feeding mode 3 < feeding mode 4,

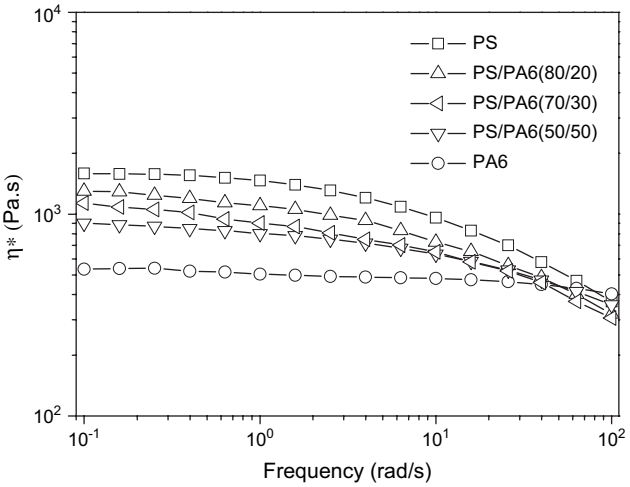

Fig. 1. Complex viscosity vs. frequency for the PS, PA6 and PS/PA6 blends (80/20, 70/30 and 50/50) blend at 230 °C.

which may further be seen from the SEM micrographs of the PS/PA6/PS-*g*-PA6 (80/20/20.6) blends from these four feeding modes (Fig. 3). When the PS-*g*-PA6 concentration was below 10%, the above order was not fully respected. Nevertheless, for both rotation speeds and over the entire PS-*g*-PA6 concentration range studied, feeding modes 2 and 4 were clearly the most and least efficient, respectively.

For a given PS/PA6 blend and a given rotation speed, the above differences in the emulsification curve among the four different feeding modes had to result mainly from differences in conditions under which the PS-*g*-PA6b emulsifier reached the PS/PA6 interfaces. From the thermodynamic viewpoint, whatever the feeding mode the final PA6 particle size would have been the same if the copolymer added to the blend had all reached the interfaces. That the PA6 particle size depended on the feeding mode implies that the amount of the PS-*g*-PA6b copolymer chains that had reached the PS/PA6 interfaces depended on the feeding mode. The fact that feeding modes 2 and 4 were the most efficient and most inefficient, respectively, implies that the former and latter feeding modes provided, respectively, the most favorable and most unfavorable conditions for the mass transfer (migration) of the PS-*g*-PA6b graft copolymer to the PS/PA6 (80/20) blend. Those results were not fully expected and remain poorly understood.

Table 7
Description of four feeding modes for the PS/PA6/PS-*g*-PA6b blends

Feeding mode designation	Description
Feeding mode 1 (one-step)	All the components (PS, PA6 and PS-*g*-PA6b) were charged to the mixer at the same time and were mixed for 8 min
Feeding mode 2 (two-step)	PS and PS-*g*-PA6b were charged to the mixer first and then PA6 4 min later. The blend was mixed for another 4 min
Feeding mode 3 (two-step)	PA6 and PS-*g*-PA6b were charged to the mixer first and then PS 4 min later. The blend was mixed for another 4 min
Feeding mode 4 (two-step)	PS and PA6 were charged to the mixer first and then PS-*g*-PA6b 4 min later. The blend was mixed for another 4 min

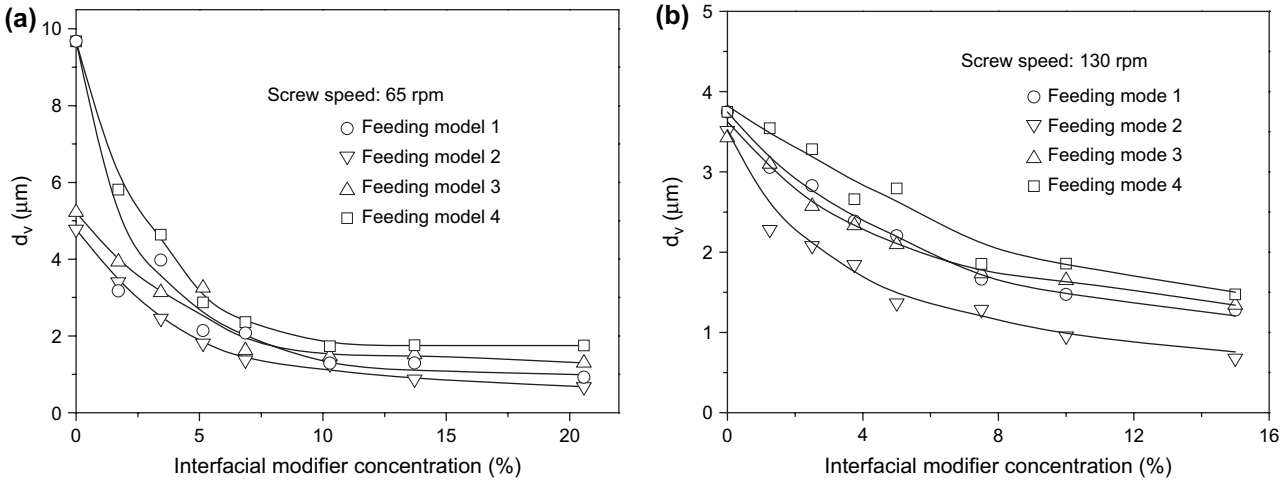

Fig. 2. Emulsification curves of the PS/PA6 (80/20) blend for four different feeding modes. The PS-*g*-PA6b concentration was based on the mass of the dispersed phase. (a) Rotation speed at 65 rpm and (b) rotation speed at 130 rpm. Mixing time: 8 min for the one-step feeding and 4 min for the two-step feeding after the last component of the blend was charged; temperature = 230 °C. Symbols: experimental data; lines: trend lines.

In the case of feeding mode 2, PS (major phase) and PS-*g*-PA6 (emulsifier) charged to and mixed in the mixer first. PA6 (minor phase) was added later when PS and PS-*g*-PA6 were completely molten. As PA6 gradually melted, the molten fraction was concomitantly dispersed in the molten mixture of PS and PS-*g*-PA6. PA6 droplets were then stabilized by PS-*g*-PA6 that was already present in the medium. In feeding mode 1, all the components of the blend were charged to the mixer at the same time. However they did not melt at the same time. PS started to melt first, followed by PS-*g*-PA6 and then PA6. From this viewpoint, feeding mode 1 was similar to feeding mode 2.

In feeding mode 3, PA6 and PS-*g*-PA6 were charged to the mixer first and PS later. To some extent, it was the opposite of

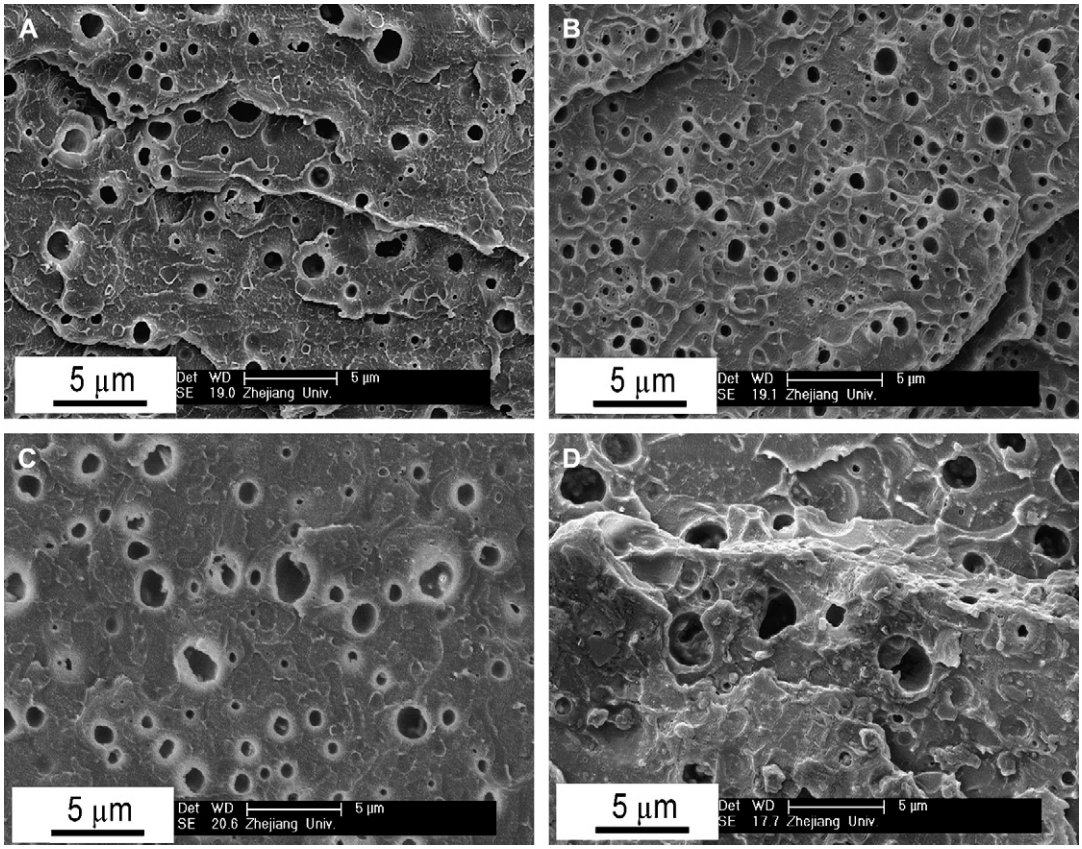

Fig. 3. SEM micrographs of microtomed surface of the PS/PA6/PS-*g*-PA6b (80/20/20.6) blend for four different feeding modes. (A) Feeding mode 1, (B) feeding mode 2, (C) feeding mode 3 and (D) feeding mode 4. Mixing time: 8 min for the one-step feeding and 4 min for the two-step feeding after the last component of the blend was charged; temperature = 230 °C.

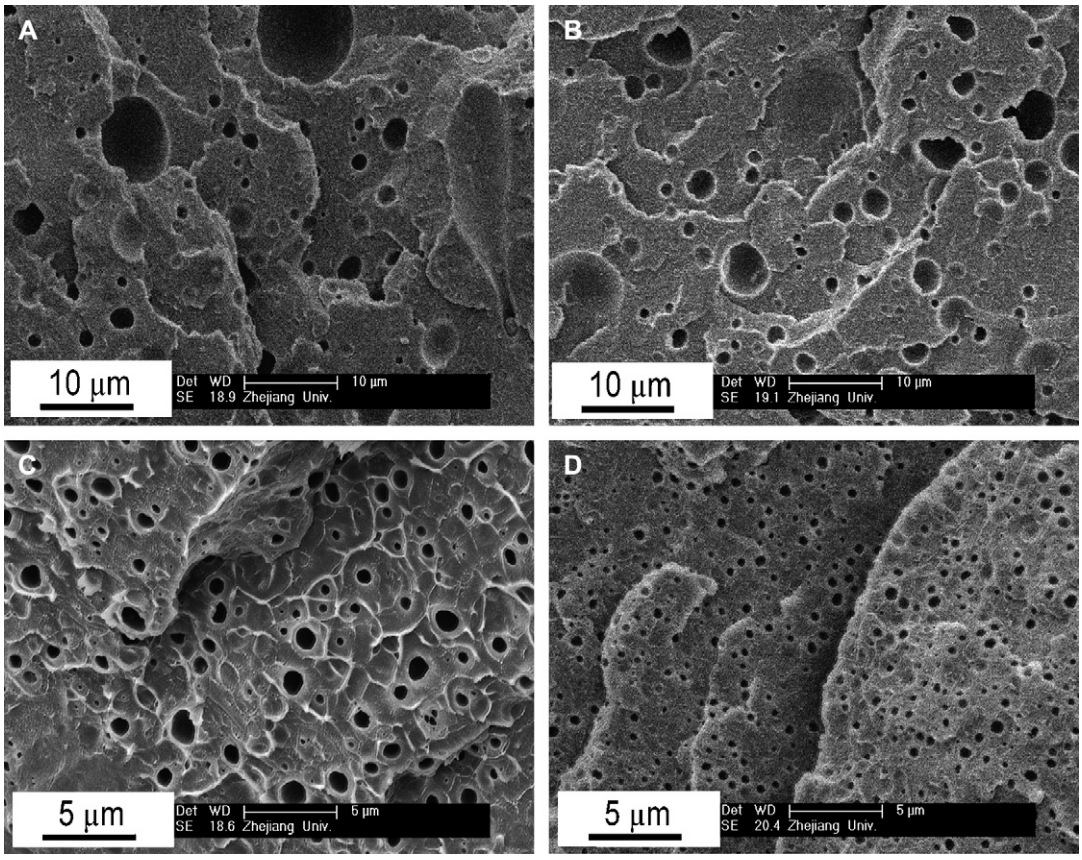

Fig. 4. SEM micrographs of microtomed surface of the PS/PA6/PS-*g*-PA6b (80/20/13.7) blend change with mixing time for feeding mode 1. Mixing temperature = 230 °C and rotation speed = 65 rpm. Mixing time: (A) 2 min, (B) 4 min, (C) 6 min, and (D) 10 min.

feeding mode 2 in terms of the feeding sequence. Since PA6 was the minor phase, the addition of PS, the major phase, necessarily led to phase inversion. The results in Fig. 2 infer that the phase inversion process might not have been good for the migration of the emulsifier to the PS/PA6 interfaces. In feeding mode 4, PS and PA6 were mixed first and the PS-*g*-PA6 emulsifier was added later. The results in Fig. 2 show that it was the worst feeding mode. The biggest difference between feeding mode 4 and the other three feeding modes was that in feeding mode 4, the PS-*g*-PA6 emulsifier was added the latest after PS and PA6 were already mixed.

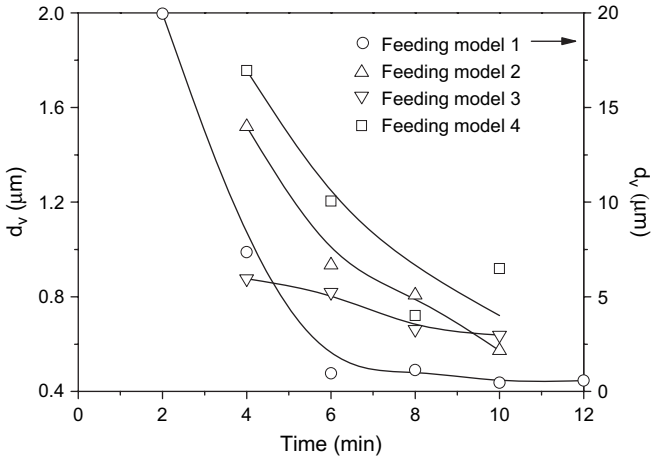

Fig. 5. Changes in the size of the dispersed phase of the PS/PA6/PS-*g*-PA6b (80/20/13.7) blend with mixing time for different feeding modes. Mixing temperature = 230 °C and rotation speed = 65 rpm. For feeding mode 1 time "0" corresponds to the moment when all the components were fed to the mixer. In the other feeding modes it corresponds to the moment when the last component was fed to the mixer, i.e., 4 min after the first two components were fed to the mixer. Symbols: experimental data; lines: trend lines.

Although detailed mechanisms that govern the morphology development of the PS/PA6/PS-*g*-PA6 blends are unclear, the above results seem to advise two rules. First, the emulsifier should be present as soon as the blending process starts (the minor phase begins to melt). Second, phase inversion should be avoided. The first rule is in line with a conclusion drawn in the literature [20]. To the authors' knowledge, the second one has not been mentioned in the literature. It should be pointed out that these two rules may not necessarily be valid for all blend systems or processing conditions. This is because many important parameters (such as the viscosity ratio of the matrix and dispersed phase, the interface tension and so on) that may affect the morphology development of polymer blends are not studied.

As pointed out above, based on the thermodynamic arguments, the final size of the dispersed phase domain should be independent of the feeding mode provided that all the copolymer chains reach the interfaces. In order that all the copolymer chains reach the interfaces, a certain amount of time was

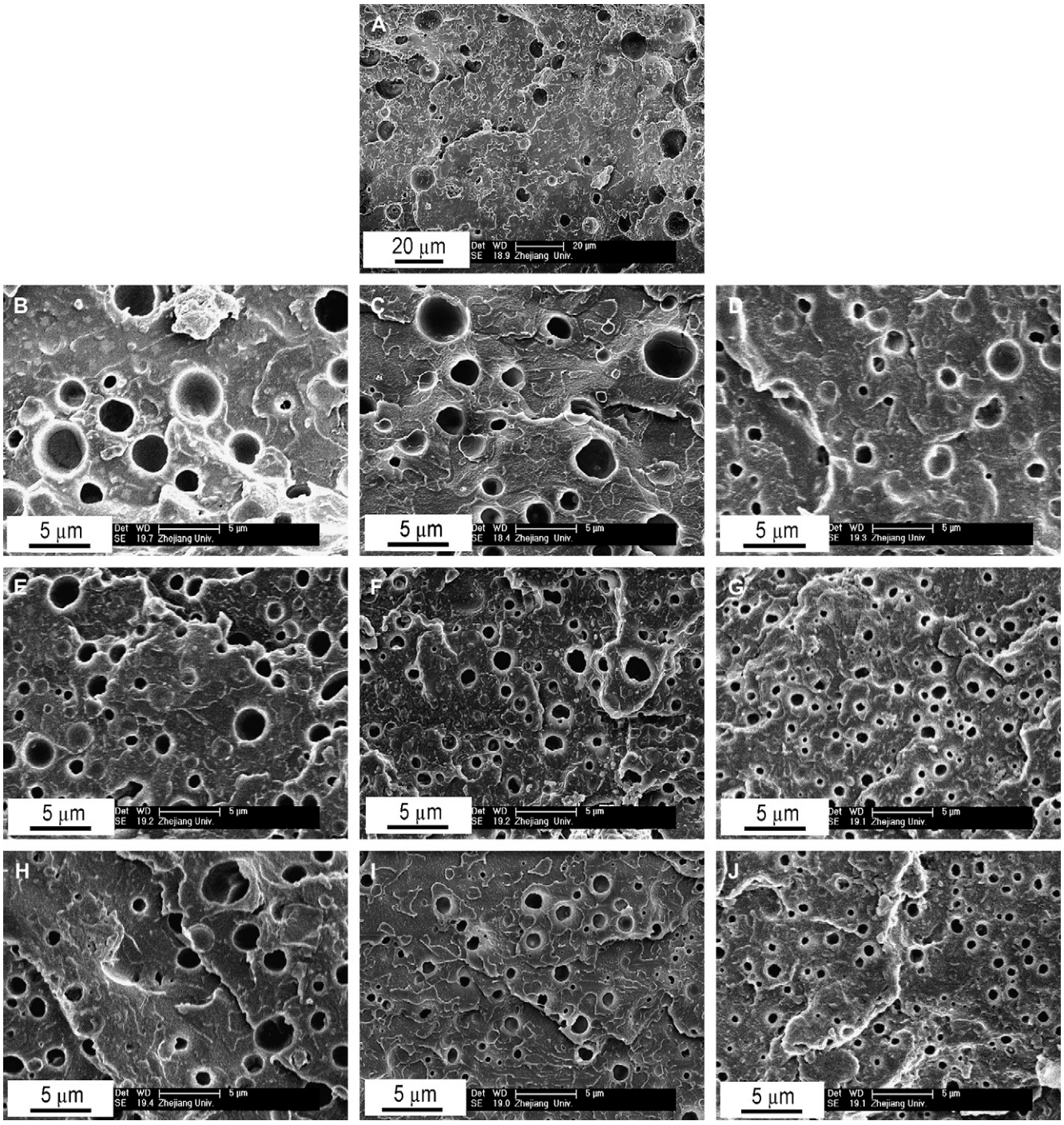

Fig. 6. SEM micrographs of microtomed surface for the various PS/PA6 (80/20) blends: (A) without PS-*g*-PA6, (B) PS-*g*-PA6a (2.2), (C) PS-*g*-PA6b (1.7), (D) PS-*g*-PA6c (1.4), (E) PS-*g*-PA6a (13.3), (F) PS-*g*-PA6b (10.3), (G) PS-*g*-PA6c (8.6), (H) PS-*g*-PA6a (17.7), (I) PS-*g*-PA6b (13.7) and (J) PS-*g*-PA6c (11.5). Mixing temperature = 230 °C, feeding mode = one-step, mixing time = 8 min, and rotation speed = 65 rpm.

necessary, which may be confirmed from the fact that the size of the dispersed phase decreased with the blending time, as shown in Fig. 4. Fig. 5 compares the four feeding modes in terms of the evolution of the PA6 particle size as a function of time for the PS/PA6/PS-*g*-PA6b (80/20/13.7) blend. It is seen that the difference was very big at short mixing time. As the mixing time increased, the difference narrowed and possibly disappeared at longer times. In other words, when the mixing time was long enough, the feeding mode itself had little effect on the final morphology. This confirms that the differences in the emulsification curve among the four different feeding modes were mostly related to differences in the speed at which the copolymer migrated to the interfaces. Since polymer blending is often carried out in a screw extruder whose residence time is normally very short, an appropriate feeding mode can be crucial for the morphology.

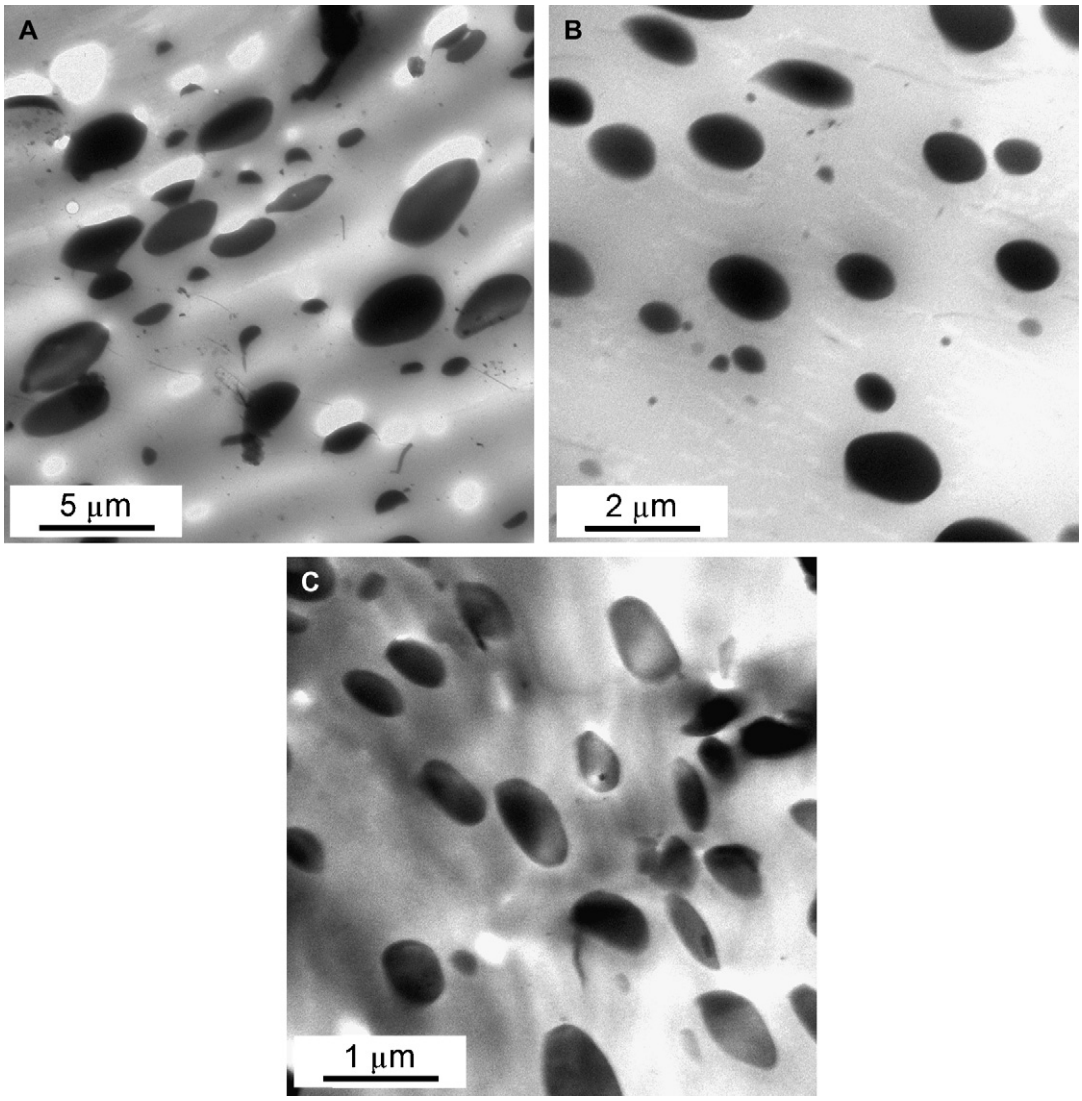

Fig. 7. TEM micrographs for various PS/PA6/PS-*g*-PA6 (80/20/*x*) blends: (A) PS-*g*-PA6a (4.4), (B) PS-*g*-PA6c (4.3), (C) PS-*g*-PA6c (8.6), where *x* is the percentage of the equivalent pure PS-*g*-PA6 with respect to the dispersed phase. Mixing temperature = 230 °C, feeding mode = one-step, mixing time = 8 min, and rotation speed = 65 rpm.

3.3. Effect of the molecular structure of the PS-g-PA6 graft copolymer

Figs. 6–8 compare, respectively, the SEM, TEM micrographs and the emulsification curves of PS/PA6 blends with PS-*g*-PA6a, PS-*g*-PA6b and PS-*g*-PA6c as the emulsifiers. Those three emulsifiers were similar in the PS backbone length and same in number of PA6 grafts but different in the PA6 graft length (see Table 5). The number-average molar mass of each PA6 graft was 1.7, 2.2 and 5.1 kg/mol for PS-*g*-PA6a, PS-*g*-PA6b and PS-*g*-PA6c, respectively. Interestingly, the longer the PA6 grafts, the smaller the final PA6 particle size, thus higher the emulsification efficiency. Moreover, PS-*g*-PA6c, the graft copolymer with the longest PA6 grafts, was by far much more efficient than PS-*g*-PA6a and PS-*g*-PA6b. Noolandi and Hong [21,22] predicted that the efficiency of a diblock copolymer to compatibilize a blend of immiscible homopolymers would increase with increasing molar mass. Longer chains would increase the thickness of the interface, which would decrease the enthalpy of the system. However, the results of Matos et al. [4], Cigana et al. [7] and Lepers and Favis [23] showed that the molar mass had little effect on the emulsification at high molar masses. Therefore, it may be deduced that in the short chain length range (perhaps below the critical entanglement length of PA6), the emulsifier length may have a significant effect on its emulsification efficiency, while its effect would be negligible at long chain length range.

Fig. 9 compares the emulsification curves between PS-*g*-PA6a and PS-*g*-PA6d. Those two emulsifiers were similar both in the PS backbone and PA6 graft lengths but different in the number of PA6 grafts (Table 5). PS-*g*-PA6a and PS-*g*-PA6d had, on average, 6.6 and 1.8 PA6 grafts per PS backbone, respectively. The results showed that their emulsification curves superimposed, indicating that the number of grafts in the PS-*g*-PA6 graft copolymer did not have a noticeable effect

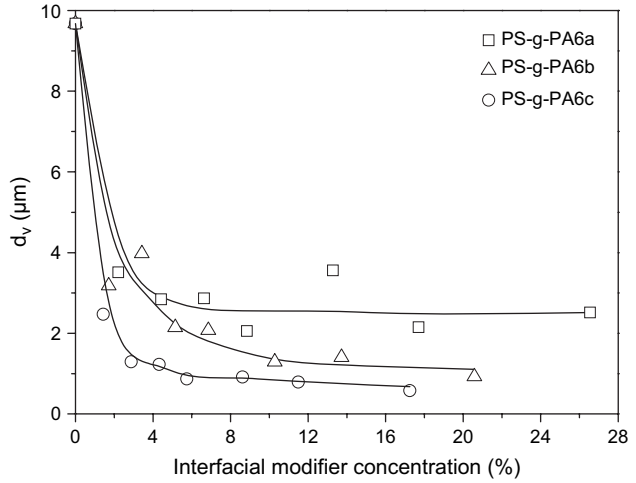

Fig. 8. Effect of the PA6 graft length of PS-*g*-PA6 on the emulsification efficiency for the PS/PA6 (80/20) blend. PS-*g*-PA6a, PS-*g*-PA6b and PS-*g*-PA6c had almost the same PS backbone length and same number of PA6 grafts but different PA6 graft lengths. Mixing temperature = 230 °C, feeding mode = one-step, mixing time = 8 min, and rotation speed = 65 rpm. Symbols: experimental data; lines: trend lines.

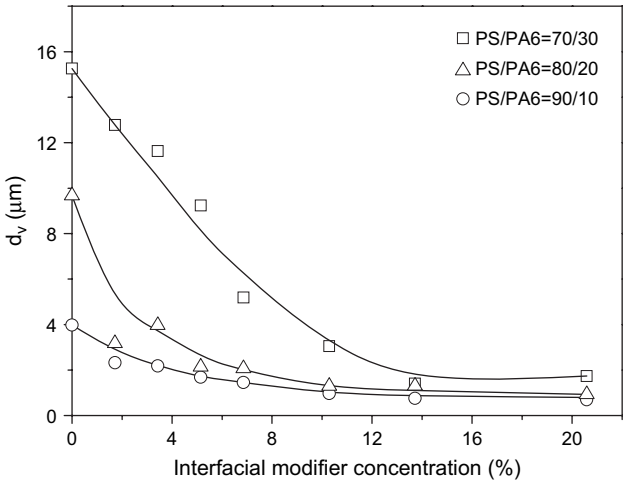

Fig. 10. Effect of the PS/PA6 blend composition on the emulsification curve. The emulsifier (PS-*g*-PA6b) concentration was based on the dispersed phase concentration. Mixing temperature = 230 °C, feeding mode = one-step, mixing time = 8 min and rotation speed = 65 rpm. Symbols: experimental data; lines: trend lines.

on the emulsification efficiency. It should be kept in mind that the PA6 grafts in PS-*g*-PA6a and PS-*g*-PA6d were very short, 1.6 or 1.7 kg/mol. Thus this conclusion might not be valid for much longer grafts.

3.4. Effect of the blend composition on the emulsification curve

Fig. 10 compares the emulsification curves for three PS/PA6 blends that differed only in the PS/PA6 mass ratio. The emulsifier was PS-*g*-PA6b. For each of the three emulsification curves, there was a critical emulsifier concentration, C_{crit}, above which the PA6 particle size did not decrease further but leveled-off. However, it was not easy to determine its value in a precise manner, especially when the dispersed phase concentration was small. Apparently, the C_{crit} values for the 90/10 and 80/20 blends were similar but slightly below the 70/30 blend. The C_{crit} for the 70/30 blend was somewhere between 13% and 14% relative to the dispersed phase composition. On the other hand, the size of the dispersed phase domains at the plateau was significantly higher for the 70/30 blend than for the 90/10 and 80/20 ones. This indicates that even if the emulsifier concentration relative to the dispersed phase concentration was high and the same, coalescence might take place when the dispersed phase concentration was high enough.

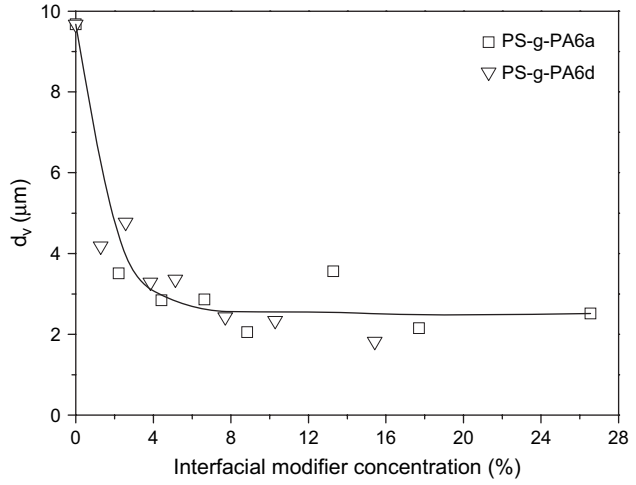

Fig. 9. Effect of the number of the PA6 grafts of the PS-*g*-PA6 on the emulsification efficiency for the PS/PA6 (80/20) blend. PS-*g*-PA6a and PS-*g*-PA6d had the same PS backbone length and same PA6 graft length but different number of PA6 grafts per PS backbone. Mixing temperature = 230 °C, feeding mode = one-step, mixing time = 8 min and rotation speed = 65 rpm. Symbols: experimental data; lines: trend lines.

4. Conclusions

In this work, a batch mixer was used to study the emulsification efficiency of graft copolymers and the effect of feeding mode on the emulsification efficiency using the emulsification curve approach. Blends were composed of polystyrene (PS) and polyamide 6 (PA6). PS was always the matrix and PA6 the dispersed phase. A series of graft copolymers of PS and PA6, denoted as PS-*g*-PA6, with different molecular structures were used as emulsifiers.

Feeding mode had a very significant effect on the size of the dispersed phase domains at short mixing time and its effect decreased or became negligible at long mixing time. At short mixing time the efficiency of four feeding modes followed the order: feeding mode 2 (PS and PS-*g*-PA6 were fed to the mixer first and PA6 later) > feeding mode 1 (PS, PA6 and PS-*g*-PA6 were fed altogether) > feeding mode 3 (PA6 and PS-*g*-PA6 were fed first and PS later) > feeding mode 4 (PS and PA6 were fed first and PS-*g*-PA6 later). This indicates

that feeding mode affected mostly the time necessary for the PS-*g*-PA6 emulsifier to reach and emulsify the PS/PA6 interfaces.

For a given feeding mode, the molecular structure of the PS-*g*-PA6 graft copolymer also had a profound effect on its emulsification efficiency. For three emulsifiers similar in the PS backbone length (33.3 kg/mol) and same in number of the PA6 grafts (6.6 grafts per PS backbone) but different in the PA6 graft length (1.7, 2.2 and 5.1 kg/mol, respectively), their emulsification efficiency increased with increasing PA6 grafts. On the other hand, there was a little difference in terms of the emulsification efficiency between two emulsifiers similar both in the PS backbone (33.3–36.9 kg/mol) and PA6 graft lengths (1.6–1.7 kg/mol) but different in the number of PA6 grafts (6.6 and 1.8 PA6 grafts per PS backbone, respectively).

For a given mass ratio between the emulsifier and the dispersed phase, the size of the dispersed phase domains increased with increasing dispersed phase concentration, indicating the occurrence of coalescence. Moreover coalescence decreased with increasing mass ratio between the emulsifier and the dispersed phase.

Acknowledgments

The authors thank the National Natural Science Foundation of China (Grant numbers 50390097 and 20310285), the Ministry of Science and Technology of China through an international cooperation program (Grant number 2001CB711203) and the Association Franco-Chinoise pour la Recherche Scientifique et Technique – AFCRST (Grant number PRA Mx02-07) for their financial support. They also thank a reviewer for her/his very useful comments.

References

[1] Baker W, Scott C, Hu GH. Reactive polymer blending. Munich: Hanser Publisher; 2001.
[2] Li T, Hiltner A, Baer E, Qurik RP. J Polym Sci Part B Polym Phys 1995;33:667.
[3] Li H, Hu GH, Sousa JA. J Polym Sci Part B Polym Phys 1999;37:3368.
[4] Matos M, Favis BD, Lomellini P. Polymer 1995;36:3899.
[5] Chio WM, Park OO, Lim JG. J Appl Polym Sci 2004;91:3618.
[6] Hong BK, Jo WH. Polymer 2000;41:2069.
[7] Cigana P, Favis BD, Jerome R. J Polym Sci Part B Polym Phys 1996;34:1691.
[8] Cigana P, Favis BD. Polymer 1998;39:3373.
[9] Harrats C, Fayt R, Jérôme R. Polymer 2002;43:863.
[10] Cimmino S, Coppola F, D'Orazio L, Greco R, Maglio G, Malinconico M, et al. Polymer 1986;27:1874.
[11] Willis JM, Favis BD. Polym Eng Sci 1988;28:1416.
[12] Lee JD, Yang SM. Polym Eng Sci 1995;35:1821.
[13] Cartier H, Hu GH. Polym Eng Sci 1999;39:996.
[14] Hu GH, Sun YJ, Lambla M. Polym Eng Sci 1996;36:676.
[15] Sun YJ, Hu GH, Lambla M, Kotlar HK. Polymer 1996;37:4119.
[16] Hu GH, Li H, Feng LF. Macromolecules 2002;35:8247.
[17] Hu GH, Li H, Feng LF. Polymer 2005;46:4562.
[18] Zhang CL, Feng LF, Hu GH, Xu ZB. J Appl Polym Sci 2006;101:1972.
[19] Li GZ, Feng LF, Gu XP, Xu ZB, Hu GH, Liu JH. J Funct Polym 2005;18:127.
[20] Li H, Hu GH. J Polym Sci Part B Polym Phys Ed 2001;39:601.
[21] Noolandi J, Hong MK. Macromolecules 1982;15:482.
[22] Noolandi J, Hong MK. Macromolecules 1984;17:1531.
[23] Lepers JC, Favis BD. AIChE J 1999;45:887.